Mon. Not. R. astr. Soc. (1991) **252,** 249–260

Symmetry breaking in stellar dynamos

R. L. Jennings and N. O. Weiss

Department of Applied Mathematics and Theoretical Physics, University of Cambridge, Cambridge CB3 9EW

Accepted 1991 May 17. Received 1991 May 16; in original form 1991 March 12

SUMMARY

The generation of magnetic fields in stars like the Sun can be described by an azimuthally averaged dynamo model. Solutions of the linear (kinematic) problem have pure dipole or quadrupole symmetry, i.e. toroidal fields that are antisymmetric or symmetric about the equator. These symmetries can only be broken at bifurcations in the non-linear regime, which lead to the appearance of spatially asymmetric mixed-mode solutions. The symmetries of dipole, quadrupole and mixed-mode solutions, whether steady or periodic, form the same group for any axisymmetric dynamo. To establish the bifurcation structure it is necessary to follow unstable as well as stable solutions. This is only feasible for simple systems and a minimal non-linear $\alpha\omega$ dynamo is studied in detail in order to illustrate the formation of mixed-mode periodic solutions and to distinguish between their symmetries. The results are applied to the Sun (where there are persistent deviations from dipole symmetry) and to other late-type stars.

1 INTRODUCTION

Cyclic magnetic activity is characteristic of slowly rotating lower main-sequence stars like the Sun. The solar magnetic field oscillates aperiodically with a mean period of about 22 yr (Stix 1989). If this field is averaged azimuthally it can be split into poloidal (meridional) and toroidal (azimuthal) components; the toroidal field reverses at sunspot minimum while the poloidal field reverses around sunspot maximum. At any epoch the magnetic field is approximately described by a toroidal field that is antisymmetric about the equatorial plane and a poloidal field that is symmetric about the equator: we refer to such a field as having dipole symmetry. The alternative parity, with a symmetric toroidal field and an antisymmetric poloidal field, is said to have quadrupole symmetry. Detailed observations show, however, that the Sun's magnetic field deviates from perfect symmetry: one hemisphere may be more active than the other and this asymmetry can persist for many cycles (Tang, Howard & Atkins 1984; Stenflo & Vogel 1986; Visozo & Ballester 1990). This paper is concerned with the origins of spatial asymmetry.

Two processes have been advanced in order to explain cyclic variations of activity in the Sun. The simpler relies on torsional oscillations with a 22-yr period in the radiative interior. These oscillations generate an alternating toroidal magnetic field, which is injected into the convective zone to produce the activity observed at the surface (e.g. Gough 1990). The second mechanism involves dynamo action near the base of the convective zone: it is more complicated but has been much more extensively investigated (e.g. Parker 1979; Zel'dovich, Ruzmaikin & Sokoloff 1983; Schüssler 1983; Weiss 1989 and references therein). The strength of the magnetic field is limited by non-linear effects and, since the Lorentz force is independent of the field's sign, any fluctuations in angular velocity should have an 11-yr period. The facts that the observed fluctuations do have an 11-yr (rather than a 22-yr) period and that the dipole field itself reverses at the surface argue in favour of a dynamo. Although the evidence is not conclusive, most comparisons have favoured this process (e.g. Cowling 1981). We shall assume here that magnetic fields in slowly rotating late-type stars are indeed maintained by hydromagnetic dynamos.

The generation of azimuthally averaged magnetic fields is conveniently described by mean field dynamo theory (Moffatt 1978; Parker 1979; Krause & Rädler 1980; Zel'dovich *et al.* 1983). In a star poloidal fields are converted into toroidal flux by differential rotation (the ω effect); then the helicity associated with cyclonic eddies twists the toroidal field to produce reversed poloidal flux (the α effect). The formal derivation of mean field dynamo equations relies on a separation of scales in space or time, which is not present in a stellar convective zone (Cowling 1981; Weiss 1983; Hoyng 1990). Nevertheless, $\alpha\omega$-dynamo models capture the essential physics and have been widely used. In stars we expect differential rotation to be symmetric about the equator, while the α effect (which depends on the Coriolis force) is antisymmetric. The eigenfunctions of the linear (kinematic) dynamo equations themselves have either dipole or quadrupole symmetry and these symmetries are preserved in the non-linear regime. Thus symmetry can only be broken at a bifurcation. In particular, stability may be

transferred from one solution branch to another (e.g. from pure quadrupole to pure dipole solutions) via an intermediate branch of mixed-mode solutions. Recent advances in non-linear dynamics (Arnol'd 1983; Guckenheimer & Holmes 1986) have made it possible to describe the underlying bifurcation structure in such problems.

To establish the bifurcation structure in a non-linear dynamo it is necessary to identify and to follow both stable and unstable solution branches, and to determine their stability. This is much easier for low-order systems of ordinary differential equations than for partial differential equations. Hence it is convenient to study truncated models which exhibit non-trivial spatiotemporal behaviour (*cf.* Nagata, Proctor & Weiss 1990). We shall devise a model that allows us to investigate the bifurcation structure associated with changes in spatial symmetry without introducing temporal chaos. Solutions are typically periodic and it is essential to confine our attention to a minimal system if we are to follow all the details of successive bifurcations. We shall, however, focus on generic results which are relevant to a wide class of dynamos.

It is widely believed that the dynamo in a G-star like the Sun is located near the base of the convective zone (Weiss 1989). Our model is constructed by flattening out the magnetic layer to give a Cartesian system, while retaining certain essential features of the spherical geometry (Stix 1972). A complete discussion of this model problem, treating its bifurcation structure in great detail, testing the accuracy at different levels of truncation and comparing different non-linear saturation mechanisms, is provided by Jennings (1991, Paper I). Here we are concerned with astrophysical implications of these results, so we need only discuss the simplest model problem. Some preliminary conclusions have already been announced (Weiss 1990; Jennings & Weiss 1990). Earlier discussions of the development of spatial structure in stellar magnetic fields had to rely on linear theory (Parker 1971; Durney, Mihalas & Robinson 1981; Rädler 1986; see also Paper I); we are able to clarify the relationship between linear growth rates and non-linear solutions. Previously published studies of non-linear dynamos have yielded stable solutions with dipole and quadrupole parity as well as mixed-mode solutions (Brandenburg *et al.* 1989a,b; Schmitt & Schüssler 1989; Moss, Tuominen & Brandenburg 1990; Rädler *et al.* 1990) but they have not included unstable solution branches. Our treatment fills this gap and allows us to exhibit the full bifurcation structure for the first time. In addition, we demonstrate that there can be more than one stable solution in certain parameter ranges.

Our idealized dynamo model is introduced in the next section, where we also classify the symmetries of the system and of steady or periodic solutions. Dynamo action arises as an instability of the trivial (field-free) solution when the relevant parameter (the dynamo number D) is increased. Linear behaviour and bifurcations from the trivial solution are summarized in Section 3. In Section 4 we include a meridional circulation in order to allow bifurcations of codimension two, where dipole and quadrupole solutions become unstable at the same value of D. Non-linear behaviour is described in Section 5; there we present numerical results for a truncated model with 14 spatial modes, where growth of the field is limited by magnetic buoyancy and quenching of differential rotation. These results exhibit the qualitative effects with which we are concerned; further details are supplied in Paper I. In the final section we discuss the implications of these calculations for stellar dynamos.

2 THE IDEALIZED MODEL AND ITS SYMMETRIES

An axisymmetric stellar magnetic field $\boldsymbol{B}$ can be split into a poloidal component $\boldsymbol{B}_P = \nabla \wedge (A\hat{\boldsymbol{\phi}})$ and a toroidal component $\boldsymbol{B}_T = B\boldsymbol{\phi}$, referred to spherical polar coordinates (r, θ, ϕ), with $A = B = 0$ at the poles ($\theta = 0, \pi$). We suppose that there is an $\alpha\omega$ dynamo located in a thin spherical shell of radius r_0, near the base of the convective zone, and that it is possible to average across this magnetic layer so as to obtain fields that are independent of r, with $A = A(\theta, t)$ and $B = B(\theta, t)$. We set $\alpha = \alpha_0 \cos\theta$ and $\omega_0 = d\Omega/dr$, where $\Omega(r)$ is the angular velocity; then the linear mean-field dynamo equations reduce to

$$\frac{\partial A}{\partial t} = \alpha_0 \cos\theta B + \frac{\eta}{r_0^2 \sin^2\theta}\left[\sin\theta \frac{\partial}{\partial\theta}\left(\sin\theta \frac{\partial A}{\partial\theta}\right) - A\right],$$

$$\frac{\partial B}{\partial t} = r_0 \omega_0 \sin\theta B_r + \frac{\eta}{r_0^2 \sin^2\theta}\left[\sin\theta \frac{\partial}{\partial\theta}\left(\sin\theta \frac{\partial B}{\partial\theta}\right) - B\right] \tag{1}$$

(Moffatt 1978; Parker 1979). Solutions of these equations can be expanded in terms of the eigenfunctions $\{P_n^1(\cos\theta), n = 1, 2, \ldots\}$ of the one-dimensional diffusion operator (Schmitt & Schüssler 1989).

This system can be further simplified by reducing it from spherical to flat Cartesian geometry, while retaining an antisymmetric α effect and ensuring that the ω effect vanishes at the poles. Thus we adopt local Cartesian coordinates (x, y, z), where x corresponds to colatitude, y increases in the azimuthal direction and the z axis points radially outward, with $\boldsymbol{B} = (0, B, \partial A/\partial x)$ and $A = A(x, t)$, $B = B(x, t)$. After rescaling, we obtain from (1) the non-dimensional system

$$\frac{\partial A}{\partial t} = D\cos x B + \frac{\partial^2 A}{\partial x^2}, \qquad \frac{\partial B}{\partial t} = \sin x \frac{\partial A}{\partial x} + \frac{\partial^2 B}{\partial x^2}, \tag{2}$$

subject to the boundary conditions

$$A = B = 0 \qquad \text{at} \qquad x = 0, \pi \tag{3}$$

(*cf.* Paper I). Equations (2) are linear and contain a single parameter, the dynamo number $D = \alpha_0 \omega_0 r_0^3/\eta^2$. For dynamo waves to propagate from the poles towards the equator (as observed in the Sun) we shall henceforth require that $D < 0$ (e.g. $\alpha_0 < 0$, $\omega_0 > 0$; see Parker 1979).

To describe non-linear behaviour we follow the procedure used in many previous studies (see, for example, Weiss, Cattaneo & Jones 1984; Paper I and references therein). Thus we represent quenching of the α effect or the ω effect by the Lorentz force by introducing arbitrary coefficients, depending only on the strength of the predominant toroidal field, such that

$$\alpha_0 \to \frac{\alpha_0}{1 + \tau B^2}, \qquad \omega_0 \to \frac{\omega_0}{1 + \kappa B^2}, \tag{4}$$

where τ and κ are arbitrary positive constants. In addition we allow for losses owing to magnetic buoyancy, on the assump-

tion that flux escapes with a velocity proportional to B^2 (Jones 1983). Then we have the model system

$$\frac{\partial A}{\partial t}=\frac{D\cos x}{1+\tau B^2}B+\frac{\partial^2 A}{\partial x^2},\quad \frac{\partial B}{\partial t}=\frac{\sin x}{1+\kappa B^2}\frac{\partial A}{\partial x}+\frac{\partial^2 B}{\partial x^2}-\lambda B^3, \quad (5)$$

with $\lambda>0$, subject to the boundary conditions (3). In their structure these equations resemble those of Stix (1972) though the latter lack the factor $\sin x$ in the second equation and differ in the form of the non-linear terms. Other one-dimensional systems have been considered by Leighton (1969), Krause & Meinel (1988), Schmitt & Schüssler (1989), Belvedere, Pidatella & Proctor (1990) and Schmalz & Stix (1991).

The system (5) with boundary conditions (3) possesses two important symmetries. The first is the dipole symmetry

$$d: \quad (x,t)\to(\pi-x,t) \qquad (A,B)\to(A,-B) \quad (6)$$

and the second is the quadrupole symmetry

$$q: \quad (x,t)\to(\pi-x,t) \qquad (A,B)\to(-A,B). \quad (7)$$

These symmetries generate a fourth-order abelian group (D_2). This includes their product

$$i=dq: \quad (x,t)\to(x,t), \qquad (A,B)\to(-A,-B), \quad (8)$$

which corresponds to a simple reversal of the field (*cf.* Nagata *et al.* 1990; Moore, Weiss & Wilkins 1991) and the identity

$$E: \quad (x,t)\to(x,t), \qquad (A,B)\to(A,B). \quad (9)$$

The equations possess a trivial solution ($A=B=0$) for all values of the parameter D; this is the only solution with the symmetry i (and the full D_2 symmetry of the system). Non-trivial solutions may possess the dipole symmetry d or the quadrupole symmetry q, which are in general mutually exclusive. At the equator ($x=\pi/2$) solutions with dipole or quadrupole symmetry satisfy the conditions

$$\frac{\partial A}{\partial x}=B=0 \quad \text{or} \quad A=\frac{\partial B}{\partial x}=0, \quad (10)$$

respectively. Solutions may also be asymmetric, possessing the trivial symmetry E but neither d nor q.

Dynamo action occurs when the trivial solution becomes unstable. The amplitude of solutions of the linear system (2) then grows exponentially with time until non-linear effects from (5) eventually become important. At the onset of instability the symmetry of the trivial solution is broken at a bifurcation, giving rise to solutions with either dipole or quadrupole symmetry. Near a stationary bifurcation there will be two branches of non-trivial steady solutions related by the symmetry i which has just been broken: hence the bifurcation must be a pitchfork (Guckenheimer & Holmes 1986).

An oscillatory (Hopf) bifurcation from the trivial solution will lead to a branch of periodic solutions with period P and the symmetry

$$t_i: \quad (x,t)\to(x,t+\tfrac{1}{2}P), \qquad (A,B)\to(-A,-B). \quad (11)$$

It follows from (6) and (11) that periodic dipole solutions have the additional symmetry

$$t_q=dt_i: \quad (x,t)\to(\pi-x,t+\tfrac{1}{2}P), \qquad (A,B)\to(-A,B), \quad (12)$$

while from (7) and (11) periodic quadrupole solutions have the symmetry

$$t_d=qt_i: \quad (x,t)\to(\pi-x,t+\tfrac{1}{2}P), \qquad (A,B)\to(A,-B). \quad (13)$$

These symmetries can only be broken at a subsequent bifurcation. To classify all the symmetries of periodic solutions we identify $t+P$ with t. Then d, q and t_i generate the eighth-order group $D_{2h}=D_2\otimes Z_2$ (*cf.* Moore *et al.* 1991) which also includes the symmetry

$$t_e=dt_d=qt_q: \quad (x,t)\to(x,t+\tfrac{1}{2}P), \qquad (A,B)\to(A,B), \quad (14)$$

possessed by steady solutions for all P. The same symmetries apply to *any* axisymmetric dynamo model.

From (3) any solution can be expanded in Fourier series of the form

$$A(x,t)=\sum_{n=1}^{N}A_n(t)\sin nx, \qquad B(x,t)=\sum_{n=1}^{N}B_n(t)\sin nx, \quad (15)$$

with N infinite. For a solution with the dipole symmetry d

$$A_n=0\ (n\ \text{even}), \qquad B_n=0\ (n\ \text{odd}) \quad (16)$$

from (6), while for a solution with the quadrupole symmetry q

$$A_n=0\ (n\ \text{odd}), \qquad B_n=0\ (n\ \text{even}) \quad (17)$$

from (7). The symmetry i implies that $A_n=B_n=0$ for all n. Periodic solutions can also be expanded as Fourier series in time such that

$$A_n(t)=\sum_{m=-\infty}^{\infty}A_{nm}\exp\left(\frac{2im\pi t}{P}\right), \qquad B_n(t)=\sum_{m=-\infty}^{\infty}B_{nm}\exp\left(\frac{2im\pi t}{P}\right). \quad (18)$$

Then

$$A_n(t+\tfrac{1}{2}P)=\sum_{m=-\infty}^{\infty}(-)^m A_{nm}\exp\left(\frac{2im\pi t}{P}\right) \quad \text{etc.} \quad (19)$$

From (11) the symmetry t_i therefore requires that $A_{nm}=B_{nm}=0$ for m even i.e. that only odd harmonics appear in the series for A_n and B_n. Similarly, t_q implies that $A_{nm}=0$ for $(m+n)$ odd and $B_{nm}=0$ for $(m+n)$ even, from (12), while t_d implies that $A_{nm}=0$ for $(m+n)$ even and $B_{nm}=0$ for $(m+n)$ odd, from (13). As expected, a sufficient condition for the symmetry t_e is that $A_{nm}=B_{nm}=0$ for $m\neq 0$.

Pure dipole oscillations possess the symmetries d, t_i and t_q, while pure quadrupole oscillations have symmetries q, t_i and t_q. Dipole symmetry can be broken at a secondary pitchfork bifurcation leading to mixed-mode solutions possessing *either* the symmetry t_q *or* the symmetry t_i alone. Breaking quadrupole symmetry similarly leads to mixed-mode solutions with *either* the symmetry t_d *or* the symmetry t_i. Hence any branch of periodic mixed-mode solutions that links a branch of pure dipole oscillations to one of pure quadrupole oscillations *must* have the symmetry t_i. Mixed-mode branches can be identified by inspecting the co-

Table 1. Symmetries of solutions.

Solution	Label	Symmetries	Non-zero coefficients A_{nm}, B_{nm}	
			Dipole	Quadrupole
Trivial		i, d, q, t_e	–	–
Steady solutions				
Dipole	ds	d, t_e, t_d	$m=0$	–
Quadrupole	qs	q, t_e, t_q	–	$m=0$
Mixed	ms	t_e	$m=0$	$m=0$
Periodic solutions				
Dipole	d	d, t_i, t_q	m odd	–
Quadrupole	q	q, t_i, t_d,	–	m odd
Mixed	mi	t_i	m odd	m odd
Mixed	mq	t_q	m odd	m even
Mixed	md	t_d	m even	m odd
Asymmetric	e	E	all m	all m

efficients A_{nm}, B_{nm} for dipole and quadrupole components. The values of m for which there are non-zero coefficients are listed in Table 1.

3 LINEAR THEORY

Both the linear equations (2) and the non-linear equations (5) have to be treated numerically. Hence we use (15) to express A and B as finite Fourier series. For the linear problem we assume that A_n, B_n vary as $\exp(st)$ and substitute from (15) into (2) to obtain the eigenvalues s. It can easily be verified that the eigenfunctions have either pure dipole or pure quadrupole symmetry, so it is only necessary to find the eigenvalues of an $N\times N$ matrix. Thus there is no difficulty in obtaining accurate results by making N sufficiently large. As N is increased, however, the non-linear problem soon becomes intractable (since we want to follow unstable periodic solutions). Hence we are forced to adopt a severely truncated expansion. In order to have linear results that are consistent with the non-linear calculations in Section 5 we therefore focus our attention on the case with $N=7$ in (15). With this crude model there are only four Fourier modes for A and three for B with dipole symmetry, or three for A and four for B with quadrupole symmetry.

Bifurcation values of $|D|$ ($D<0$) are listed in Table 2, both for $N=7$ and for $N=15$. With $N=7$ the first bifurcation is a pitchfork (QS_1: $s=0$), followed by a Hopf bifurcation (DO_1: $s=\pm 4.6$i), leading to a branch of periodic solutions with dipole symmetry. Then comes a second stationary bifurcation (QS_2) and a Hopf bifurcation (QO_1: $s=\pm 3.7$i), leading to quadrupole solutions. Comparison with results for $N=15$ shows that the order of the bifurcations is preserved and that bifurcation values have converged for $|D|<300$.

The steady quadrupole mode is an anomaly. Its growth rate rises to a low maximum, passes through zero at the second pitchfork bifurcation (QS_2) and becomes positive again at the third (QS_3). Meanwhile the eigenfunction develops a more complicated spatial structure. This curious mode, first identified by Parker (1971), is a feature of one-dimensional dynamo models (Stix 1972; Schmitt & Schüssler 1989; Schmalz & Stix 1991). Accurate calculations of the growth rate show that it oscillates indefinitely about zero with ever-decreasing amplitude as $|D|$ is increased (Parker 1971, 1979; Schmitt & Schüssler 1989). Although steady solutions have appeared in various $\alpha\omega$ dynamos they are sensitive to geometrical assumptions on which the models are based (*cf.* Rädler 1986; Jennings *et al.* 1990 and Paper I).

The growth rates ($\mathscr{R}s$) of the oscillatory modes increase monotonically as $|D|$ is increased (see Paper I). The principal dipole and quadrupole modes that bifurcate at DO_1 and QO_1 have the largest growth rates; higher modes vary on smaller spatial scales and are consequently damped. For large values of $|D|$ the growth rates of the two principal modes become approximately equal. As $|D|$ increases the corresponding eigenfunctions gradually develop a more complicated spatial structure.

4 MERIDIONAL CIRCULATION: CODIMENSION-TWO BEHAVIOUR

In this section we explore the effects of adding additional terms to the linear equations (2) in order to represent a quadrupole meridional circulation. There are two reasons for doing this: first, we can see whether the primary bifurcations are model-dependent or robust; secondly, by adjusting two parameters (the dynamo number D and the normalized amplitude, R, of the meridional flow) we can investigate bifurcations of codimension two that occur when two primary bifurcations coincide. These multiple bifurcations act as organizing centres for non-linear behaviour in their neighbourhoods of parameter space.

There is some evidence for a weak meridional circulation with quadrupole symmetry in the Sun (e.g. Wöhl 1990). Advection of the field by such circulations, which preserves the symmetries of the dynamo equations, has been included in several kinematic $\alpha\omega$-dynamo models (e.g. Roberts 1972; Roberts & Stix 1972). In axisymmetric spherical geometry it can easily be shown that a solenoidal flow cannot act as a dynamo on its own, i.e. that the field decays if the α effect is switched off (e.g. Moffatt 1978). To preserve this result in one-dimensional Cartesian geometry we construct linear equations of the form

$$\frac{\partial A}{\partial t}=D\cos xB-R\left(\sin 2x\frac{\partial A}{\partial x}+\cos 2xA\right)+\frac{\partial^2 A}{\partial x^2},$$
$$\frac{\partial B}{\partial t}=\sin x\frac{\partial A}{\partial x}-R\left(\sin 2x\frac{\partial B}{\partial x}+\cos 2xB\right)+\frac{\partial^2 B}{\partial x^2}. \qquad (20)$$

Eigenfunctions still have either dipole or quadrupole symmetry and if $D=0$ it follows from (20) and (3) that

$$\frac{d}{dt}\int_0^\pi A^2\,dx=-R\int_0^\pi\frac{\partial}{\partial x}(\sin 2xA^2)\,dx+2\int_0^\pi A\frac{\partial^2 A}{\partial x^2}\,dx$$
$$=-2\int_0^\pi\left(\frac{\partial A}{\partial x}\right)^2 dx\le 0. \qquad (21)$$

Table 2. Bifurcation values of $|D|$ for different modes and their sensitivity to discretization.

N	QS_1	QS_2	QS_3	QO_1	DO_1	DO_2
7	9	246	474	273	102	1152
15	9	241	668	264	102	2097

Thus the poloidal field decays in the absence of an α effect and eventually the toroidal field must likewise decay.

The bifurcation values in Table 2 are altered when $R \neq 0$. Fig. 1 shows the positions of bifurcations in the *RD* plane, computed with $N=16$. The most relevant quadrant is that with $R>0$ (pole-to-equator circulation) and $D<0$, where the relevant bifurcations correspond to those labelled QS_1, QS_2, QO_1 and DO_1 in Table 1. Here the stationary bifurcations disappear for $R>2$, leaving only oscillatory dipole and quadrupole modes. On the other hand, steady dipole (DS) modes appear for $R<-2.6$ and also for $D>15$.

We can identify three significant codimension-two bifurcations in the half-plane $D<0$. The first is that at $R\approx -0.2$, $D\approx -245$, where the stationary and oscillatory quadrupole bifurcations coincide. At this multiple bifurcation there is a double zero eigenvalue; behaviour nearby is described by the normal form equation for a Bogdanov bifurcation with reflectional (Z_2) symmetry (Arnol'd 1983). We expect to find two branches of steady solutions emerging from the pitchfork bifurcation and a branch of oscillatory solutions emerging from the Hopf bifurcation, and the oscillatory branch typically terminates either in a secondary Hopf bifurcation or in a heteroclinic bifurcation (Knobloch & Proctor 1981). There is a similar bifurcation affecting dipole solutions at $R\approx -2.6$, $D\approx -110$, which happens to be close to a turning point on the DS bifurcation curve.

Finally, there is another double bifurcation at a much higher value of $|D|$, where the two Hopf bifurcations coincide. This occurs at $R\approx 6.48$, $D\approx -2530$ with $N=16$ and at $R\approx 7.07$, $D\approx -3280$ with $N=128$. The remarkable feature of this bifurcation is that the dipole and quadrupole modes have almost identical frequencies (to within 2 per cent). Normally we might expect to find quasiperiodic (doubly periodic) mixed-mode solutions in the neighbourhood of a double Hopf bifurcation (Guckenheimer & Holmes 1983) but here there is likely to be a strong resonance so that mixed-mode solutions will be periodic.

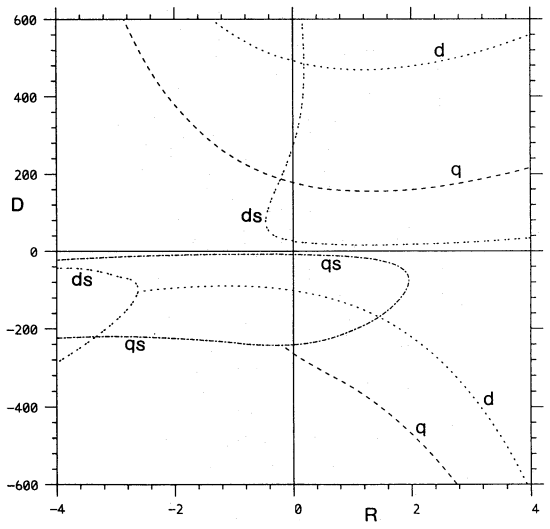

Figure 1. Curves of marginal stability in the *RD* plane for oscillatory and steady modes of each parity (labelled as in Table 1) for the kinematic problem with meridional circulation. Since all modes are unstable when $D=0$ it is straightforward to deduce the change of stability associated with each curve. Bifurcations from the trivial solution in Fig. 2 lie along the line $R=0$ for $D<0$.

The actual bifurcation patterns near the codimension-two points depend on the form of the non-linear terms in the equations. In the next section we shall see that the existence of these multiple bifurcations helps to explain the behaviour of non-linear solutions even when $R=0$.

5 NON-LINEAR RESULTS

We have obtained numerical solutions of the non-linear system (5), with no meridional circulation, for $D<0$ and various choices of non-linear saturation mechanism. The equations can be solved as an initial-value problem by a collocation method: once the Fourier series (15) have been substituted into (5) the linear terms can be obtained directly. Then a fast Fourier transform is used to synthesize A and B at N independent, equally-spaced mesh points, with $x=j\pi/(N+1)$, $j=1, 2,\ldots,N$, so that non-linear terms can be evaluated directly and transformed back by a second FFT. We found it convenient to choose either $N=7$ or $N=15$, so that there were 8 or 16 intervals in the range $0\le x\le\pi$, with $x=\pi/2$ as a collocation point. This procedure allows us to follow stable solutions as parameters are varied.

Steady or periodic solutions can be obtained using second-order iterative processes based on Newton's method, regardless of whether they are stable or unstable. To investigate their stability we perturb these solutions and compute the relevant eigenvalues (see Paper I).Thus we can follow branches of steady and periodic solutions and so establish the full bifurcation structure for our idealized model problem. Note, however, that computational requirements rapidly become prohibitive as N is increased. Hence we have chosen to explore behaviour with $N=7$ systematically and to check selected results at higher resolution with $N=15$.

The choice of saturation mechanism in our model is largely a matter of taste. In Gilman's (1983) self-consistent dynamo calculation the velocity shear was reduced by the magnetic field. Moreover, observations show that the angular velocity fluctuates during the solar cycle (Ulrich *et al.* 1988). Flux loss by magnetic buoyancy (Leighton 1969; Hughes & Proctor 1988) could be an important process, while many models have relied on α quenching, although there is inevitably no observational evidence for this mechanism. We choose to keep buoyancy losses and quenching of differential rotation only, setting $\kappa=\lambda$ and $\tau=0$. Without loss of generality we may then set $\kappa=\lambda=1$ in (5). For steady solutions we then compute the mean square toroidal field

$$\langle B^2\rangle=\frac{1}{\pi}\int_0^{\pi}B^2\,dx \qquad \text{or} \qquad \langle B^2\rangle=\frac{1}{\pi P}\int_0^{P}\int_0^{\pi}B^2\,dx\,dt, \quad (22)$$

for steady or periodic solutions respectively, as a measure of dynamo activity.

We represent the bifurcation structure by plotting $\langle B^2\rangle$ as a function of the stability parameter $|D|$ for stable and unstable solutions. Fig. 2 shows a schematic bifurcation diagram in which the ordering of bifurcations is preserved. This is our principal result. Solutions with dipole or quadrupole symmetry, as well as solutions that are asymmetric, all lie on branches which start or terminate in bifurcations. All the branches shown have been followed numerically and we believe that the diagram is complete. Full lines indicate stable solutions and broken lines denote unstable solutions. It is

immediately apparent that the bifurcation structure cannot be interpreted without reference to the unstable branches. In what follows we analyse this structure in some detail, emphasizing those features that we expect to be robust.

The first non-trivial solution appears at QS_1 (*cf.* Table 2) so we shall restrict our attention initially to solutions that possess the quarupole symmetry q of (7). The supercritical pitchfork bifurcation at QS_1 gives rise to a symmetrical pair of stable steady quadrupole solutions lying on the branch labelled *qs* in Fig. 2. The steady branch *qs* extends from QS_1 to a second pitchfork bifurcation at QS_2; later it reappears at the third pitchfork bifurcation QS_3. The branch of periodic solutions, labelled q, emerges from a subcritical Hopf bifurcation at QO_1 and has a turning point (corresponding to a saddle-node bifurcation) at $|D|=217$, where it becomes stable to perturbations with quadrupole symmetry. The q branch then continues to arbitrarily high values of $|D|$.

The saddle-node bifurcation on the oscillatory branch q occurs before the pitchfork at QS_2. Moreover, the steady branch *qs* undergoes two Hopf bifurcations at $|D|=215$, 222 giving rise to a short branch of periodic solutions which retain the symmetry q. This bifurcation pattern is sketched in Fig. 3(b) and the signs of the real parts of the two relevant eigenvalues (which refer only to perturbations with the symmetry q) are indicated in the figure. Such behaviour suggests that the steady and oscillatory branches are related, as indeed they are in Fig. 1. The interactions between these branches can be explained by referring back to the co-dimension-two bifurcation there. In the immediate neighbourhood of that bifurcation ($0<R+0.2\ll 0.2$) we expect to find the bifurcation pattern shown in Fig. 3(c). Here there are two oscillatory branches: the first (q_1) terminates in a Hopf bifurcation from the steady branch (Knobloch & Proctor 1981; Arnol'd 1983) but this is preceded by a secondary Hopf bifurcation leading to a second branch (q_2) of oscillatory solutions which persists to higher values of $|D|$. As the Hopf bifurcation Q_1 moves away from QS_2 (e.g. as a consequence of increasing R in Fig. 1) the oscillatory branches reconnect, producing the bifurcation pattern sketched in Fig. 3(b) for $R=0$. Eventually the two branches become independent, as in Fig. 3(a). As R is decreased, on the other hand, the Hopf bifurcation at SQ_1 disappears. For $R<0.2$ we would therefore expect to find the pattern in Fig. 3(d): the secondary Hopf bifurcation is still there and the branch q_2 of periodic solutions remains. This transition illustrates the dangers of using linear theory to predict behaviour in the non-linear regime, which can be qualitatively different: the Hopf bifurcation at QO_1 may disappear but the oscillatory branch continues to exist.

There are no steady solutions with dipole symmetry for $D<0$. The first branch of pure dipole solutions (labelled d in Fig. 2) emerges from a supercritical Hopf bifurcation at DO_1. The value of $\langle B^2\rangle$ increases monotonically with increasing $|D|$ along this branch and it remains stable to perturbations that possess the symmetry d. A second oscillatory dipole branch bifurcates much later at DO_2. Solutions on this branch correspond to octupole modes; they have much lower amplitude and are unstable to perturbations with dipole symmetry d.

Symmetry breaking leads to mixed-mode solutions which possess neither dipole nor quadrupole symmetry so that the Fourier expansions (15) of A and B contain both odd and even terms. We consider now the transfer of stability from the *qs* branch to the branch d of oscillatory dipole solutions. The steady quadrupole solutions lose stability in a supercritical Hopf bifurcation at $|D|=137$, where the symmetry q is broken. Near this bifurcation there are stable mixed-mode

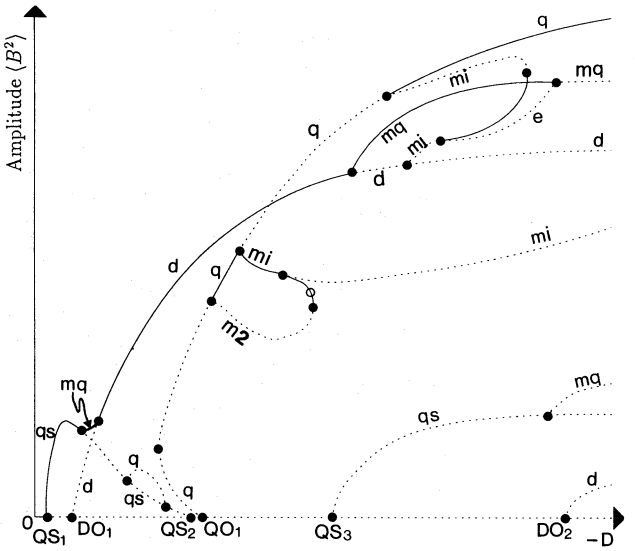

Figure 2. Bifurcation diagram for the case $\kappa=\lambda$, $\tau=0$ and $D<0$. For clarity the diagram is not to scale, but the relative amplitudes of different solutions and the order in which bifurcations occur are correct. The classification of the different branches is as in Table 1, while the branch labelled $m2$ corresponds to a quasiperiodic mixed mode solution. Local and global bifurcations are indicated by ● and ○ respectively.

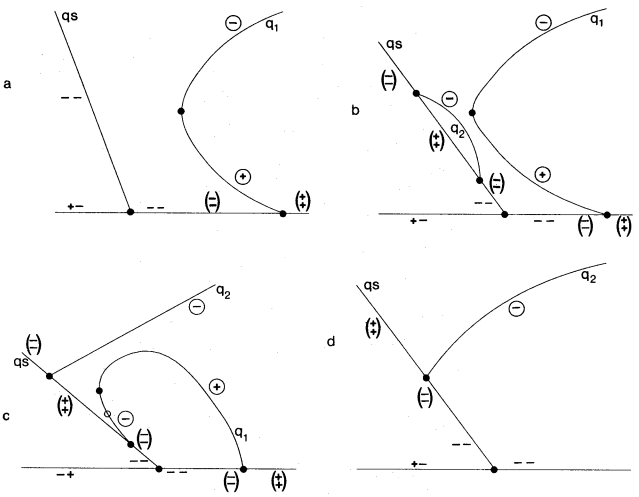

Figure 3. Bifurcation patterns at different values of R in the vicinity of the codimension-two point at $(-0.2, -240)$ in the RD plane of Fig. 1, where the oscillatory and steady quadrupole modes are simultaneously excited. (a) R sufficiently large and positive that the branch *qs* of steady solutions and the branch q_1 of periodic solutions are independent; (b) $R=0$: a pair of Hopf bifurcations lead to a second oscillatory branch, q_2 (as found numerically; see Fig. 2); (c) $0\ll R+0.2\ll 0.2$: the oscillatory branches have reconnected; (d) $R<0.2$: only the q_2 branch remains. The stability of each branch to quadrupole perturbations is indicated, with ⊕ (⊖) indicating unstable (stable) periodic solutions and brackets enclosing the real parts of complex conjugate eigenvalues.

solutions which oscillate about the unstable quadrupole solution: they lie on the branch labelled *mq* in Fig. 2, which meets branch *d* in a pitchfork bifurcation at $|D| = 180$. At this bifurcation the dipole symmetry *d* is broken, so the mixed-mode solutions retain only one of the symmetries t_i, t_q. To determine which we note from Table 1 that only solutions with the symmetry t_q have quadrupole modes with *m* even and are able to join the steady quadrupole branch with $m = 0$. Hence the oscillatory quadrupole component on the *mq* branch has half the period of the dipole component.

Now the oscillatory dipole solutions on branch *d* are already unstable to perturbations with quadrupole symmetry at the Hopf bifurcation DO_1, so they only acquire stability at the pitchfork bifurcation. Pure dipole oscillations then remain stable until $|D| = 502$, when the symmetry *d* is broken at a second pitchfork bifurcation. Stability is then transferred to mixed-mode solutions lying on a branch labelled *mq* in Fig. 2, which again possess the symmetry t_q alone. This branch remains stable to $|D| \approx 1000$, where the last remaining symmetry t_q is broken in a subcritical pitchfork bifurcation; later it regains stability in a third pitchfork bifurcation at $|D| \approx 3600$. Complicated behaviour near the last two pitchforks is described in Paper I.

Since the Hopf bifurcation at QO_1 is preceded by that at DO_1, pure quadrupole solutions on branch *q* initially have a pair of eigenvalues with positive real parts, corresponding to dipole perturbations. Between $|D| = 317$ and $|D| = 336$ lie a sequence of bifurcations associated with a strong resonance (see Paper I). Their net effect is that one real eigenvalue becomes negative and a branch of unstable mixed-mode oscillations is formed. Solutions on this branch (labelled *mi*) have the symmetry t_i only. The second eigenvalue on branch *q* passes through zero in a subcritical pitchfork bifurcation at $|D| = 659$; the branch (*mi*) of unstable mixed-mode oscillations emerging from this bifurcation links branches *q* and *d* and therefore has the symmetry t_i which is common to both (see Table 1). Stable quadrupole oscillations exist for $659 < |D| \lesssim 11\,300$. Symmetry is then lost in a subcritical pitchfork bifurcation.

The rich bifurcation structure in Fig. 2 shows the way in which stability is transferred from one branch to another, allowing an unstable branch to gain stability at a bifurcation. For certain parameter values there are two or three stable solutions, such with its own basin of attraction; a trajectory will be attracted to one or other of these depending on the initial conditions. We have stressed the distinction between pure dipole or quadrupole solutions and mixed-mode solutions with less spatial symmetry. Breaking the symmetry of a pure dipole oscillation leads to periodic solutions with the symmetries t_q or t_i, while breaking quadrupole symmetry gives solutions with symmetries t_d ot t_i. We have found examples of oscillations that exhibit the symmetries t_q and t_i; to obtain t_d we would need to study cases with $D > 0$.

A convenient way of displaying the symmetry properties of these solutions is to generate butterfly diagrams with contours of $B(x, t)$. Figs 4–7 illustrate the different symmetries that we have found. In Fig. 4(a) and (b) we show examples of pure dipole (*d*) and quadrupole (*q*) solutions. In both cases the toroidal field has the symmetry t_i of (11). Fig. 5(a) shows a mixed-mode periodic solution of type *mq* with the symmetry t_q. The field still has a predominantly dipole structure but the equatorial symmetry is broken. In the

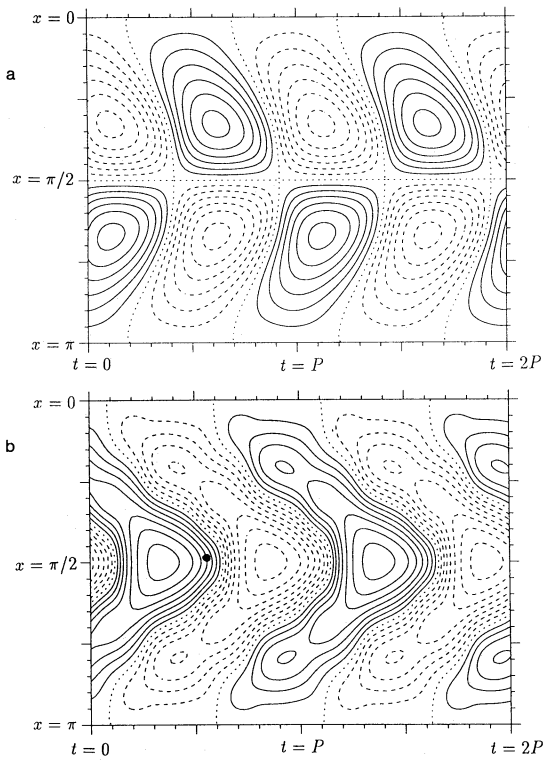

Figure 4. Contours of $B(x, t)$ (butterfly diagrams) for pure parity periodic solutions, (a) dipole, type *d* and (b) quadrupole, type *q*. Solid (broken) lines represent positive (negative) field, and a dotted contour indicates where the field is zero. Note the different symmetries about the equator ($x = \pi/2$).

immediate neighbourhood of the equator the field retains the same sign throughout (as it would for a steady quadrupole solution). There is of course an equivalent solution in which the sign of the toroidal field is reversed. The relationship between these two solutions is clarified in Fig. 5(b), which shows periodic orbits projected from the 14-dimensional phase space on to the B_2B_1-phase plane. The dipole component B_2 oscillates with reversals of sign while the quadrupole component executes oscillations of much smaller amplitude without reversing its sign. The two periodic solutions are related by the symmetry *d*, which was broken at the bifurcation from the pure dipole branch; this corresponds to reflection about the line $B_1 = 0$. The symmetry t_q ensures that each limit cycle is symmetric about $B_2 = 0$.

Fig. 6 shows solutions of type *mi*, with symmetry t_i. By contrast with Fig. 5, the field in Fig. 6(a) is predominantly quadrupolar, with stronger activity in one 'hemisphere' than in the other. The corresponding phase portraits in Fig. 6(b) show two limit cycles related by the broken symmetries *q* or *d*. Both dipole and quadrupole components reverse sign during the oscillation, so the orbits have point symmetry about the origin. In this case the amplitude of the dipole component is half that of the quadrupole component. Fig. 6(c) shows a butterfly diagram for a more extreme case, with almost all the activity of one sign at any epoch (as for an oscillatory quadrupole). The phase portraits in Fig. 6(d) retain the symmetries of Fig. 6(b) but the amplitude of the dipole component is now three times greater than that of the quadrupole.

Finally, the example in Fig. 7 shows a field of type *e*, which is strictly periodic but has no other symmetry. Close inspection of Fig. 7(a) shows that adjacent butterfly wings are all slightly different. There are now four equivalent solutions related by the symmetries that have been broken, as shown by the four distinct limit cycles in Fig. 7(b) which are related by reflection about either $B_1 = 0$ or $B_2 = 0$. In this case the field is predominantly dipolar and the fluctuations in B_2 are still relatively small.

All non-linear results described so far were obtained with $N = 7$ and are affected by discretization. We have investigated bifurcations from the pure dipole and quadrupole branches with $N = 15$ (see Paper I) and find that the structure is preserved. All the bifurcations shown in Fig. 2 for $|D| < 400$ occur in approximately the same positions but those in which stability is transferred from the *d* branch to the *q* branch are deferred to much higher parameter values

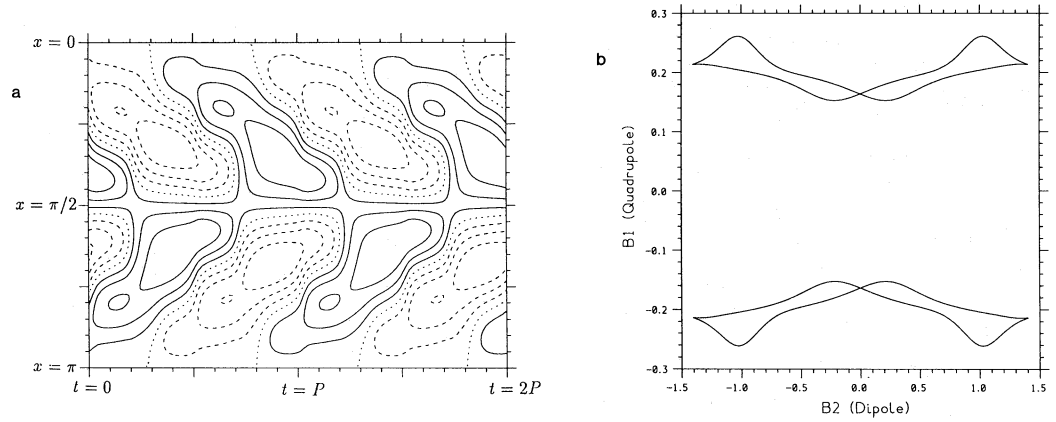

Figure 5. Periodic mixed-mode solutions of type *mq* with symmetry t_q. (a) Butterfly diagram for a predominantly dipolar solution. (b) Phase portraits in the $B_2 B_1$ plane, showing two periodic orbits related by the symmetry *d*.

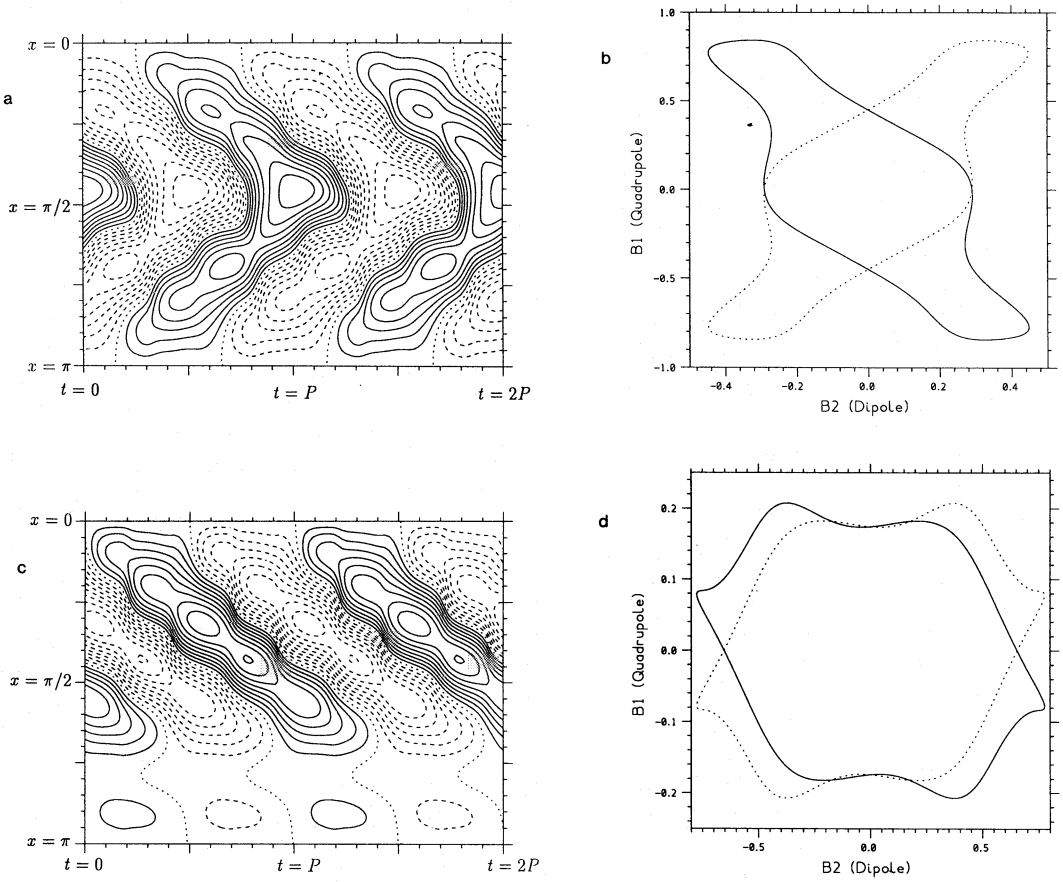

Figure 6. As Fig. 5, but for solutions of type *mi* with symmetry t_i. (a) Butterfly diagram for a predominantly quadrupolar solution with (b) corresponding phase portraits related by the symmetry *q* (or *d*). (c) and (d) Butterfly diagram and phase portraits for a solution with extreme asymmetry about the equatorial plane.

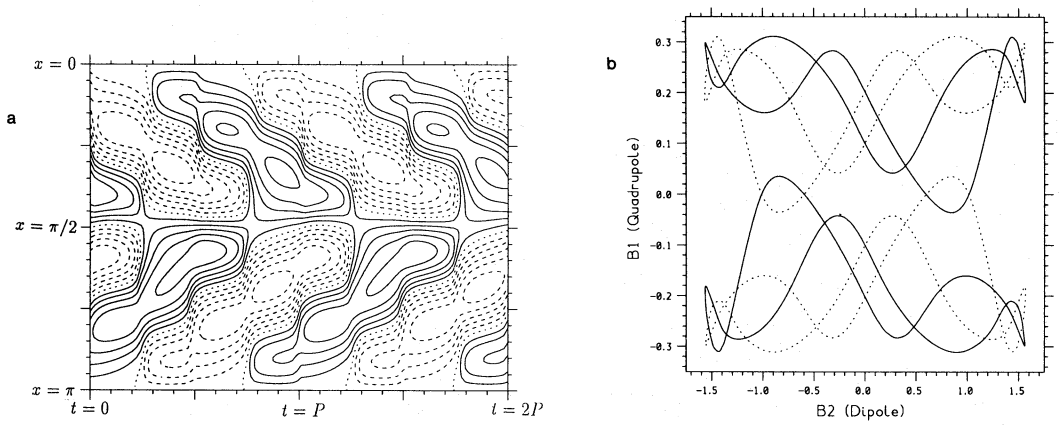

Figure 7. As Fig. 5, but for an asymmetric periodic solution of type *e*. (a) Butterfly diagram and (b) phase portraits for four solutions related by the broken symmetries.

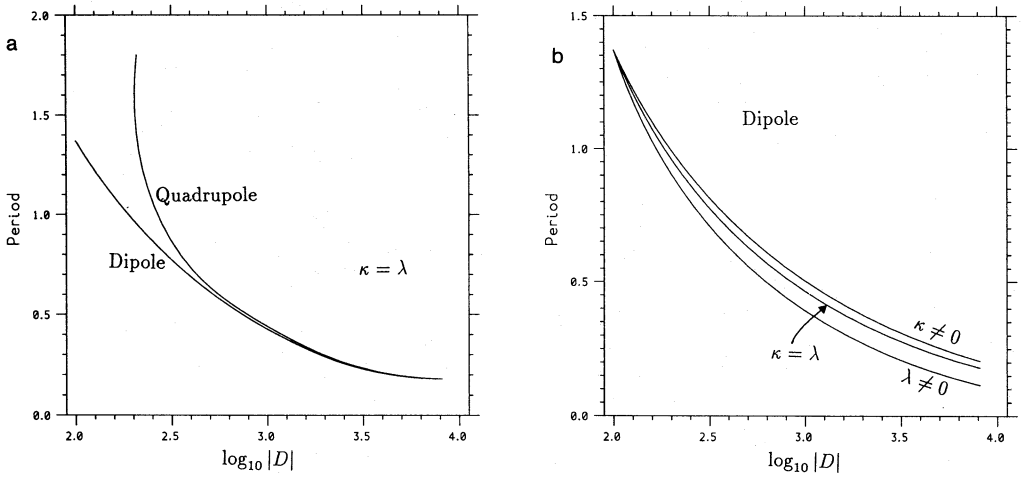

Figure 8. Variation of the period P with the dynamo number $|D|$ for (a) the primary oscillatory dipole and quadrupole solutions (marginal at DO_1 and QO_1 in Fig. 2 respectively) in the case $\kappa = \lambda$, $\tau = 0$; (b) primary oscillatory dipole solutions for three different non-linearities; $\kappa \neq 0$ (ω quenching only), $\kappa = \lambda$, $\tau = 0$ (buoyancy losses and ω quenching but no α quenching) and $\lambda \neq 0$ (buoyancy losses only).

($|D| \approx 2500$). We have not attempted to discover whether these bifurcation points converge for larger values of N. Fig. 8(a) shows the variation with $|D|$ of the period P of the pure dipole and quadrupole solutions for $N = 15$. Both periods decrease monotonically with increasing $|D|$ and tend towards the same values for large $|D|$. These curves can be fitted by a power law of the form

$$P \approx 23.4|D|^{-0.61}. \tag{23}$$

We have also explored the effects of changing the non-linear saturation mechanisms. With $\lambda \neq 0$ and $\tau = \kappa = 0$ (buoyancy losses only) or $\kappa \neq 0$ and $\tau = \lambda = 0$ (quenching of differential rotation only) the bifurcation structures differ only slightly from that described above (see Paper I). Fig. 8(b) shows P as a function of $|D|$ for the three cases with $\tau = 0$ ($\kappa = \lambda$, $\kappa = 0$ and $\lambda = 0$). There is apparently a continuous transition from one case to another and, surprisingly, there is very little difference between them. Various forms of α quenching have been studied in several other calculations. We have looked at the case with $\tau \neq 0$ and $\kappa = \lambda = 0$ (quenching of the α effect only) and find that behaviour is very different: the steady quadrupole solution remains stable at least up to $|D| = 20\,000$ and steady mixed-mode solutions appear at saddle-node bifurcations. Combining α quenching with ω quenching leads to quasiperiodic oscillations, as described in Paper I.

6 STELLAR DYNAMOS

In studying an extremely simple model problem we have emphasized those qualitative features that we expect to be generic. In particular, the symmetry properties of both steady and periodic solutions are shared by an axisymmetric dynamo. The relationship between our model and other $\alpha\omega$ dynamos is discussed in Paper I. Although those models do not necessarily reproduce the bifurcation structure shown in Fig. 2 we can still use that structure to illustrate general properties of linear and non-linear dynamo solutions.

Our results confirm a familiar warning: it is dangerous to extrapolate from a linear to a non-linear regime. The first mode to become unstable is not necessarily preferred. In Fig. 2 stability is rapidly transferred from steady quadrupole to oscillatory dipole solutions. A better procedure is to look for the linear modes with the largest growth rates. That is also unreliable but here it works well. The principal dipole and quadrupole oscillatory modes have the largest linear growth rates (which approach each other for large $|D|$) and non-linear behaviour is dominated by interactions between these modes. As $|D|$ is increased more and more dipole and quadrupole modes, with increasingly complex spatial structure, bifurcate from the trivial solution. It is tempting to suppose that these unstable modes develop to become responsible for fields with complicated spatial structure in the non-linear regime (*cf.* Parker 1971; Durney *et al.* 1981). This resembles Landau's picture of turbulence, where successive Hopf bifurcations give rise to behaviour with many frequencies and many spatial scales. But that is not what happens: after the first bifurcation almost all branches bifurcating from the trivial solution are unstable. Hopf proposed a more sophisticated picture, where subsidiary bifurcations lead to multiply periodic (quasiperiodic) mixed-mode solutions with complicated spatial structures. Subsequently it was realized that the attractors could be chaotic. So turbulence is an extreme manifestation of spatiotemporal chaos.

The model problem shows the importance of following solution branches into the non-linear regime, where mixed modes appear as spatial symmetries are broken at bifurcations. Although the pattern of subsidiary bifurcations in Fig. 2 is fairly complicated the essential interactions involve only two basic solutions, on branches emerging from Hopf bifurcations at DO_1 and QO_1. In this problem more complicated spatial structures develop continuously as the dynamo number is increased, without involving the branches that emerge from subsequent bifurcations at DO_2 etc. There is an analogy with the behaviour of convection in a narrow container: two-dimensional Rayleigh–Bénard or thermosolutal convection, for example, is dominated by interactions between single-roll and two-roll solutions (e.g. Moore *et al.* 1991) and in three-dimensional convection small-scale structures appear as instabilities of boundary layers rather than as global instabilities of the whole convecting layer.

An interesting feature of the mixed-mode solutions is that they are periodic (with limit cycles) rather than quasiperiodic (with trajectories on a torus in phase space). According to standard theory (Guckenheimer & Holmes 1986) two interacting Hopf bifurcations should lead to doubly periodic solutions unless there is a resonance between frequencies at the bifurcations. In Section 4 we found a codimension-two bifurcation, where two Hopf bifurcations coincide, with $|D| \gg 1$, and the frequencies of pure dipole and quadrupole oscillations are almost equal. That is consistent with the non-linear results in Fig. 6(a). The fact that no quasiperiodic solutions appear in Fig. 2 (except for one torus associated with a different resonant interaction in the interval $319 \leq |D| \leq 336$) can be ascribed to the effects of this resonance. Stable quasiperiodic solutions do appear with other choices of parameters (e.g. $\kappa = 2\tau$, $\lambda = 0$); Brandenburg *et al.* (1989a) found a transition from a limit cycle with dipole symmetry via mixed-mode solutions lying on a torus to a quadrupolar limit cycle in a non-linear spherical dynamo model.

Of course the system (5) only captures a very limited range of physical effects. In particular, there is no dynamical coupling between the magnetic field and the fluid motion. Introducing a third equation to describe the evolution of α or the differential rotation would immediately allow more complicated dynamics, including the possibility of temporal chaos (Kleeorin & Ruzmaikin 1981; Weiss *et al.* 1984; Schmalz & Stix 1991). We have intentionally excluded such effects in order to concentrate on spatial structure. More realistic dynamo models lead to complicated spatiotemporal patterns that are difficult to analyse (e.g. Gilman 1983).

In conclusion, we attempt to apply our findings to stellar dynamos. In slowly rotating stars we expect that the dynamo number $|D| \propto \Omega^2$ (Durney & Latour 1978; Noyes, Weiss & Vaughan 1984b). Two-dimensional calculations suggest that dynamo action sets in at a Hopf bifurcation leading to modes with pure dipole symmetry. In old stars that are rotating very slowly we would therefore hope to see azimuthally averaged magnetic fields with the symmetry *d*. The solar magnetic field is predominantly dipolar (Stenflo & Vogel 1986) but there is clear evidence of north–south asymmetry. Tang *et al.* (1984) report that the magnetic flux emerging in the northern hemisphere exceeds that in the southern hemisphere by about 10 per cent, while Visozo & Ballester (1990) found a comparable asymmetry in sunspot areas. These asymmetries have persisted for at least three cycles, though they may change in sign and magnitude on a longer time-scale. The most pronounced N–S asymmetry occurred at the end of the Maunder minimum: of 56 sunspots recorded between 1671 and 1713 all but two were in the southern hemisphere (Spörer 1889). These observations imply that dipole symmetry is broken in the Sun and suggest that the solar dynamo is of type *mi* with symmetry t_i, resembling the example in Fig. 6(c), but modulated aperiodically in time.

The same result should hold for other G-stars with ages similar to the Sun's and rotation periods of about 25 d. There are several examples of cyclic activity with periods around 10 yr in such stars, though the pattern of magnetic activity is not uniquely determined by the rotation rate and structure of the star. We have seen in Fig. 2(a) that there may be several stable solutions for the same value of $|D|$. This is a typical feature of non-linear problems and similar behaviour has been reported in other dynamo models too (Brandenburg *et al.* 1989a,b). Soderblom & Baliunas (1988) give examples of binary stars where the components have similar masses but show very different paterns of activity although their ages are identical.

Increasing the control parameter $|D|$ corresponds to following the Sun's evolution backwards in time, reversing the spindown caused by magnetic braking. Stars rotating slightly faster than the Sun (with rotation periods greater than about 10 d) should show qualitatively similar behaviour. With increasing non-linearity we expect to find more pronounced asymmetry, more complicated spatial structure and greater temporal irregularity. From Fig. 8 we see that the mean period of the oscillation decreases with increasing $|D|$. Thus we should expect to find shorter cycle periods in more rapidly rotating stars (Noyes *et al.* 1984b). Although there are only a dozen slow rotators with clear cycles like the Sun's, their behaviour suggests that P decreases with increas-

ing Ω. Noyes *et al.* found that $P \propto \Omega^{-1.25}$, though there is considerable scatter and others have criticized this result (Baliunas & Vaughan 1985); on the assumption that $|D| \propto \Omega^2$ this power law is surprisingly close to that in (23). As we have seen from Fig. 8(b), the exponent is not sensitive to the non-linear saturation mechanism. Although the period of simple dynamo waves remains constant if growth is limited by quenching α or ω (Noyes *et al.* 1984b; Weiss *et al.* 1984), our results show that ω quenching leads to standing waves with a period that decreases with increasing $|D|$. The discrepancy probably arises because the simple dynamo waves had the same spatial form for all values of D, while our new solutions develop a more complicated structure and therefore have a shorter ohmic decay time. Furthermore, the ω quenching in (5) depends on the local value of $|B|$, while quenching for dynamo waves was uniform in space and time. Our results show that the quenching mechanism cannot be identified by comparing the observed relationship between P and Ω with one-dimensional dynamo models (though two-dimensional spherical models might prove more useful).

The observed increase of magnetic activity in rapidly rotating lower main-sequence stars (Noyes *et al.* 1984a; Baliunas & Vaughan 1985) is consistent with theoretical predictions but it is not clear how far one can safely extrapolate from the behaviour of the Sun (Weiss 1989). As Ω increases the Coriolis force becomes dominant in the convective zone, affecting not only the convection pattern but also differential rotation (Knobloch, Rosner & Weiss 1981). In particular, we might expect Ω to be constant on cylindrical surfaces in the convective zone (Gilman 1979; Glatzmaier 1985) rather than a function of latitude only, as indicated by rotational splitting of p-mode frequencies in the Sun (Dziembowski, Goode & Libbrecht 1989). Moreover, the magnetic field may itself compete with Coriolis effects in determining the structure of convection (Zel'dovich *et al.* 1983; Jones, Roberts & Galloway 1990; Jones & Roberts 1990).

The simple models described here are certainly inadequate for ultra-rapid rotators with periods of less than a day, which are magnetically extremely active. They include dMe stars as well as young G stars in clusters like αPer or the Pleiades. Sunspots reduce the solar luminosity by less than 0.1 per cent but starspots may occupy 40 per cent of the surface area of an active star, while up to 80 per cent of the remaining area may be covered by intense fields of 2000 G (Baliunas & Vaughan 1985; Hartmann & Noyes 1987). So convection must be dominated by the magnetic field. In a situation where the Lorentz force, the Coriolis force and buoyancy forces are globally comparable (as in the Earth's core) behaviour may be very different; indeed, it is not clear whether the observed variations of activity correspond to cyclic reversals of the field or merely to fluctuations about a quasipermanent magnetic state.

ACKNOWLEDGMENTS

We thank Chris Jones, David Moss and Andrew Soward for many helpful comments and suggestions. This project grew out of the GFD Summer Program at Woods Hole Oceanographic Institution and benefitted from Edward Spiegel's advice. Part of the research was done by RLJ at the Department of Mathematics and Statistics, University of Newcastle-upon-Tyne. Both authors are grateful for support from SERC while this research was done.

REFERENCES

Arnol'd, V. I., 1983. *Geometrical methods in the theory of ordinary differential equations,* Springer, Berlin.
Baliunas, S. L. & Vaughan, A. H., 1985. *Ann. Rev. Astr. Astrophys.,* **23,** 379.
Belvedere, G., Pidatella, R. M. & Proctor, M. R. E., 1990. *Geophys. Astrophys. Fluid Dyn.,* **51,** 263.
Brandenburg, A., Tuominen, I. & Moss, D., 1989a. *Geophys. Astrophys. Fluid Dyn.,* **49,** 129.
Brandenburg, A., Krause, F., Meinel, R., Moss, D. & Tuominen, I., 1989b. *Astr. Astrophys.,* **213,** 411.
Cowling, T. G., 1981. *Ann. Rev. Astr. Astrophys.,* **19,** 115.
Durney, B. & Latour, J., 1978. *Geophys. Astrophys. Fluid Dyn.,* **9,** 241.
Durney, B., Mihalas, D. & Robinson, R. D., 1981. *Publs Astr. Soc. Pacif.,* **93,** 537.
Dziembowski, W. A., Goode, P. R. & Libbrecht, K. G., 1989. *Astrophys. J. Lett.,* **337,** L53.
Gilman, P. A., 1979. *Astrophys. J.,* **231,** 284.
Gilman, P. A., 1983. *Astrophys. J. Suppl. Ser.,* **53,** 243.
Glatzmaier, G. A., 1985. *Astrophys. J.,* **291,** 300.
Gough, D. O., 1990. *Phil. Trans. Roy. Soc. Lond. A,* **330,** 627.
Guckenheimer, J. & Holmes, P., 1986. *Nonlinear oscillations, dynamical systems and bifurcations of vector fields,* 2nd printing, Springer, New York.
Hartmann, L. W. & Noyes, R. W., 1987. *Ann. Rev. Astr. Astrophys.,* **25,** 271.
Hoyng, P., 1990. In: *Solar photosphere: structure, convection and magnetic fields,* p. 359, ed. Stenflo, J. O., Kluwer, Dordrecht.
Hughes, D. W. & Proctor, M. R. E., 1988. *Ann. Rev. Fluid Mech.,* **20,** 187.
Jennings, R. L., 1991. *Geophys. Astrophys. Fluid Dyn.,* **57,** 147 (Paper I).
Jennings, R. L. & Weiss, N. O., 1990. In: *Solar photosphere: structure, convection and magnetic fields,* p. 355, ed. Stenflo, J. O., Kluwer, Dordrecht.
Jennings, R. L., Brandenburg, A., Moss, D. & Tuominen, I., 1990. *Astr. Astrophys.,* **230,** 463.
Jones, C. A., 1983. In: *Stellar and planetary magnetism,* p. 159, ed. Soward, A. M., Gordon & Breach, London.
Jones, C. A. & Roberts, P. H., 1990. *Geophys. Astrophys. Fluid Dyn.,* **55,** 263.
Jones, C. A., Roberts, P. H. & Galloway, D. J., 1990. *Geophys. Astrophys. Fluid Dyn.,* **53,** 183.
Kleeorin, N. I. & Ruzmaikin, A. A., 1981. *Geophys. Astrophys. Fluid Dyn.,* **17,** 281.
Knobloch, E. & Proctor, M. R. E., 1981. *J. Fluid Mech.,* **108,** 291.
Knobloch, E., Rosner, R. & Weiss, N. O., 1981. *Mon. Not. R. astr. Soc.,* **197,** 45P.
Krause, F. & Meinel, R., 1988. *Geophys. Astrophys. Fluid Dyn.,* **43,** 95.
Krause, F. & Rädler, K.-H., 1980. *Mean-field magnetohydrodynamics and dynamo theory,* Pergamon, Oxford.
Leighton, R. B., 1969. *Astrophys. J.,* **156,** 1.
Moffatt, H. K., 1978. *Magnetic field generation in electrically conducting fluids,* Cambridge University Press, Cambridge.
Moore, D. R., Weiss, N. O. & Wilkins, J. M., 1991. *J. Fluid Mech.,* submitted.
Moss, D., Tuominen, I. & Brandenburg, A., 1990. *Astr. Astrophys.,* **228,** 284.
Nagata, M., Proctor, M. R. E. & Weiss, N. O., 1990. *Geophys. Astrophys. Fluid Dyn.,* **51,** 211.
Noyes, R. W., Hartmann, L. W., Baliunas, S. L., Duncan, D. K. & Vaughan, A. H., 1984a. *Astrophys. J.,* **279,** 763.

Noyes, R. W., Weiss, N. O. & Vaughan, A. H., 1984b. *Astrophys. J.*, **287,** 769.
Parker, E. N., 1971. *Astrophys. J.*, **164,** 491.
Parker, E. N., 1979. *Cosmical Magnetic Fields,* Clarendon Press, Oxford.
Rädler, K.-H., 1986. *Astron. Nachr.*, **307,** 89.
Rädler, K.-H., Wiedemann, E., Brandenburg, A., Meinel, R. & Tuominen, I., 1990. *Astr. Astrophys.*, **239,** 413.
Roberts, P. H., 1972. *Phil. Trans. Roy. Soc. Lond. A,* **224,** 663.
Roberts, P. H. & Stix, M., 1972. *Astr. Astrophys.*, **18,** 453.
Schmalz, S. & Stix, M., 1991. *Astr. Astrophys.*, **245,** 654.
Schmitt, D. & Schüssler, M., 1989. *Astr. Astrophys.*, **223,** 343.
Schüssler, M., 1983. In: *Solar and stellar magnetic fields: origins and coronal effects,* p. 213, ed. Stenflo, J. O., Reidel, Dordrecht.
Soderblom, D. R. & Baliunas, S. L., 1988. In: *Secular solar and geomagnetic variations in the last 10,000 years,* p. 25, eds Stephenson, F. R. & Wolfendale, A. W., Kluwer, Dordrecht.
Spörer, G. 1889. *Verh. Ksl. Leopoldinisch-Carolinischen Deutschen Akad. Naturforsch.*, **53,** 283.
Stenflo, J. O. & Vogel, M., 1986. *Nature,* **319,** 285.
Stix, M., 1972. *Astr. Astrophys.*, **20,** 9.
Stix, M., 1989. *The Sun,* Springer, Berlin.
Tang, F., Howard, R. & Adkins, J. M., 1984. *Solar Phys.*, **91,** 75.
Ulrich, R. K., Boyden, J. E., Webster, L., Snodgrass, H. B., Padilla, S. P., Gilman, P. & Shieber, T., 1988. *Solar Phys.*, **117,** 291.
Visozo, G. & Ballester, J. L., 1990. *Astr. Astrophys.*, **229,** 540.
Weiss, N. O., 1983. In: *Stellar and planetary magnetism,* p. 115, ed. Soward, A. M., Gordon & Breach, London.
Weiss, N. O., 1989. In: *Accretion disks and magnetic fields in astrophysics,* p. 11, ed. Belvedere, G., Kluwer, Dordrecht.
Weiss, N. O., 1990. *Phil. Trans. R. Soc. Lond. A,* **330,** 617.
Weiss, N. O., Cattaneo, F. & Jones, C. A., 1984. *Geophys. Astrophys. Fluid Dyn.*, **30,** 305.
Wöhl, H., 1990. *Publ. Debrecen Obs.*, **7,** 19.
Zel'dovich, Ya. B., Ruzmaikin, A. A. & Sokoloff, D. D., 1983. *Magnetic fields in astrophysics,* Gordon & Breach, London.